

Fast Electron Generation by Long Pulse Laser

H. Sakagami¹, T. Johzaki², T. Nakamura², H. Nagatomo², K. Mima²

¹*Department of Simulation Science, National Institute for Fusion Science, Toki, Japan*

²*Institute of Laser Engineering, Osaka University, Osaka, Japan*

1. Introduction

In the FIREX-I (Fast Ignition Realization Experiment phase-I) project, an Au cone-guided cryogenic DT target is imploded by the present Gekko XII laser system and its compressed core is heated by the LFEX (Laser for Fusion Experiment) laser with 10[kJ]/10[ps]. The goal of FIREX-I is to substantiate that the imploded core can be heated up to the ignition temperature, 5[keV]. However, efficient heating mechanisms and achievement of such high temperature have not been clarified yet. Thus we must estimate scheme performance of the fast ignition prior to new experiments, and we have been promoting the Fast Ignition Integrated Interconnecting code (FI³) project [1,2]. Under this project, the Arbitrary Lagrangian Eulerian radiation-hydro code (PINOCO), the collective Particle-in-Cell code (FISCOF), and the relativistic Fokker-Planck code (FIBMET) are integrated to understand overall physics in the fast ignition with data exchanges.

To explore FIREX-I experiments with simulations, the heating laser is set to $\lambda_L=1.06[\mu\text{m}]$, $\tau_{\text{rise}}=375[\text{fs}]$, $\tau_{\text{flat}}=5[\text{ps}]$, $\tau_{\text{fall}}=375[\text{fs}]$, and $I_L=10^{20}[\text{W}/\text{cm}^2]$, and we introduce the preformed Au plasma with real mass, $A=197$ and $Z=30$, which is estimated from an average ionization degree of Au calculated by PINOCO. Since the scale length of the preformed Au plasma affects the ion dynamics, it is assumed to have an exponential profile of the scale length (L_f) 1, 2, 3, 5 and 10 [μm] with density from $0.1n_{\text{cr}}$ up to $500n_{\text{cr}}$ (n_{cr} is the critical density), followed by the Au cone tip plasma (10[μm] width and $500n_{\text{cr}}$). To compare with previous simulation results [3], we put the imploded CD plasma (real mass, $A=7$, $Z=3.5$, 50[μm] width and $500n_{\text{cr}}$) behind the Au cone tip instead of the DT plasma. The energy of fast electrons is observed at the middle of the Au cone tip.

As the heating pulse duration is long enough even for the Au plasma to be pushed and compressed by the Ponderomotive force, it is completely plunged into a main part of the Au cone plasma and the profile steepening occurs at the laser front. The heating laser, then, directly interacts with the sharp edge plasma, whose density is much over critical and

increases in time as compression goes on. This is expected to reduce the fast electron beam intensity, hence to lead less core heating.

2. Fast Electron Beam Intensity and Electron Density

Fast electrons are mainly generated by so-called relativistic J x B heating [4] near the critical density point. This generation mechanism is due to the oscillating component of the Ponderomotive force of the laser, and it depends on the large gradient of the laser field at the interaction region. The ultrahigh intense laser also generates the higher pressure than the plasma pressure, even for extremely overdense plasmas. As the temporal pulse length is long enough for Au ions even with real mass, the Au plasma is pushed by the light pressure and snowplowed to higher density. The profile steepening also occurs; hence the laser directly interacts with the sharp edge plasma. The density at the interaction region increases as compression goes on, and this leads to shorten a skin depth of the laser. The short skin depth means a short acceleration distance and reduce the generation of fast electrons. Time evolutions of fast electron beam intensity and electron density at the laser-plasma interaction front for different scale lengths are shown in Fig. 1. It is found that the fast electron beam intensity decreases when the electron density increases.

The oscillating Ponderomotive force on electrons is given by [5]

$$f_p = -\frac{\partial}{\partial x} \left(\frac{mv_{osc}^2}{2} \frac{4\omega_L^2}{\omega_{pe}^2} e^{-2\omega_{pe}x/c} \left[\frac{1 + \cos 2\omega_L t}{2} \right] \right) \propto \left(\frac{v_{osc}^2}{c^2} \right) \omega_L^2 \left(\frac{c}{\omega_{pe}} \right). \quad (1)$$

The magnitude of the force is proportional to c/ω_{pe} , namely $(n_{cr}/n_e)^{(1/2)}$. As the electron density goes up, less fast electrons are generated by the weakened force and the beam intensity is also reduced. Fast electron beam intensity as a function of electron density at the interaction front is shown in Fig. 2 for different scale lengths. As the underdense plasma is swept away from the interaction region and the laser immediately irradiates the snowplowed plasma, the beam intensity well scales as the inverse square root of the electron density independent of the scale length of the preformed plasma.

3. Fast Electron Energy Spectrum and Core Heating

Snap shots of the fast electron energy spectrum are shown in Fig. 3 for $L_t=1$ and $10[\mu\text{m}]$. In the case of the short scale length, fast electrons are generated in early time. However the underdense plasma is swept away and the electron density at the interaction region increases quickly, the fast electron energy drops with time. On the other hand, fast electrons must

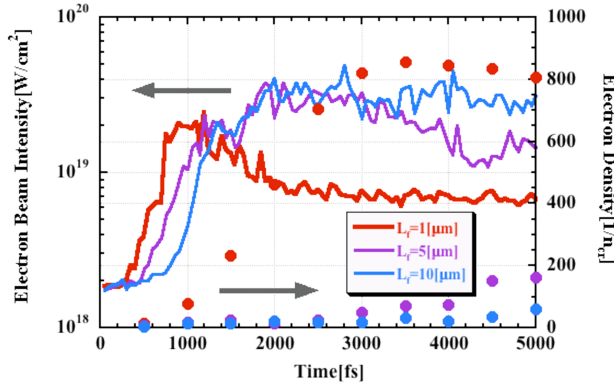


Fig. 1 Time evolutions of fast electron beam intensity (solid lines) and electron density at the laser-plasma interaction front (circles). The color of red, purple and blue indicates the scale length of 1, 5 and 10[μm], respectively.

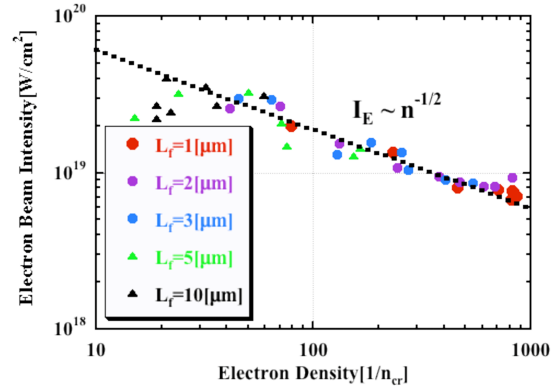


Fig. 2 The fast electron beam intensity as a function of the electron density at the interaction front. Red, purple, blue, light green and black indicate the scale length of 1, 2, 3, 5 and 10[μm], respectively.

propagate a long distance from the laser-plasma interaction region in the long scale length case, and they do not reach the observation point at 1[ps]. After that, fast electrons start to be observed and they preserve the energy spectrum even in late time because the electron density at the interaction region does not increase so much.

As the core heating is greatly affected by the fast electron energy spectrum, hence the scale length of the preformed plasma, we have performed FI³ integrated simulations to estimate core temperatures. Time evolutions of core temperatures, which are averaged over the dense region ($\rho > 10$ [g/cm³]), are shown in Fig. 4 for different scale lengths. It is noted that τ_{flat} is expanded to 10[ps] to fit FIREX-I experiments. In the case of the short scale length, the average core temperature quickly rises but shortly saturates because the fast electron beam intensity decreases. But the beam intensity and the energy spectrum of fast electrons are maintained and the core heating is sustained for a long time in the long scale length case, the core reaches higher average temperature.

When the intensity of the heating laser is extremely high, we should coat the Au cone with low-density materials (such as aerogel) to prevent the increase of the electron density for efficient core heating. If the scale length of the preformed plasma is short, we should use the relatively low intensity and long pulse laser also to prevent the increase of the electron density. However, if the pulse is too long, the core may disassemble before it is well heated. So the optimum intensity and pulse length may exist. Comparing with previous simulation results [3], we emphasize, finally, that characteristic of the dependence of core heating on the scale

length of the preformed plasma in short pulse heating lasers is completely different from that in long pulse heating lasers.

Acknowledgments

This work was supported by MEXT, the grant-in Aid for Creative Scientific Research (15GS0214).

References

- [1] H. Sakagami and K. Mima, Laser Part. Beams **22**, 41-44 (2004).
- [2] H. Sakagami, et al., Laser Part. Beams, **24**, 191-198 (2006).
- [3] T. Johzaki, et al., Proc. 33rd EPS Conf. on Plasma Physics, **P1.016** (2006).
- [4] W. L. Kruer and K. Estabrook, Phys. Fluids **28**, 430-432 (1985).
- [5] S. C. Wilks and W. L. Kruer, IEEE J. Quantum Electronics **33**, 1954-1968 (1997).

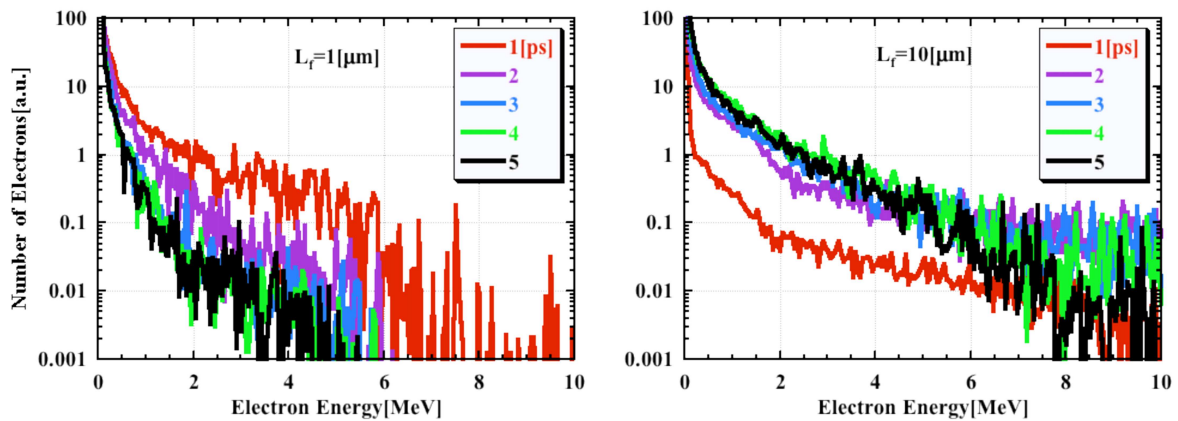


Fig. 3 Time Evolution of fast electron energy spectrum for $L_r=1$ and $10[\mu\text{m}]$. Red, purple, blue, light green and black indicate observation time of 1, 2, 3, 4 and 5[ps], respectively.

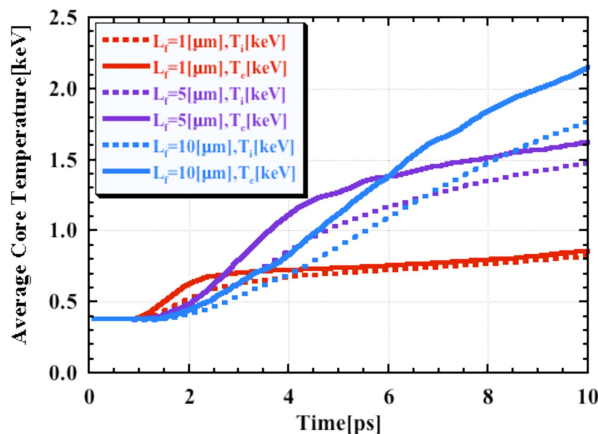


Fig. 4 Time Evolution of average core temperatures of electrons (solid lines) and ions (dash lines) for $\rho > 10[\text{g}/\text{cm}^3]$. The color of red, purple and blue indicates the scale length of 1, 5 and $10[\mu\text{m}]$, respectively.